



## USING CFD SIMULATIONS TO IMPROVE THE MODELING OF WINDOW DISCHARGE COEFFICIENTS

Erin L. Hult<sup>1</sup>, Gianluca Iaccarino<sup>2</sup>, and Martin Fischer<sup>2</sup>

<sup>1</sup> Lawrence Berkeley National Laboratory, Berkeley, CA

<sup>2</sup> Stanford University, Stanford, CA

### ABSTRACT

Accurate parameterization of flow through window openings is necessary in order to model passive and mixed-mode ventilation strategies using airflow network models and energy simulation tools. In these tools, little guidance is typically provided on selecting airflow parameters such as the discharge coefficient for windows. Detailed computational fluid dynamics (CFD) simulations can provide an inexpensive, flexible method for developing such parameterizations. In this study, the discharge coefficient for pivoted windows is considered, using analytical and CFD modeling as well as comparison with previous data. The discharge coefficient parameterization currently used in EnergyPlus can lead to an underestimate of flow through pivoted windows by up to factor of 2. This parameterization for the discharge coefficient as a function of window angle and aspect ratio is modified, and Reynolds-averaged numerical simulations are used to validate this new formulation. Analytical and numerical results compare well with measurements from window manufacturers.

### INTRODUCTION

Passive and mixed-mode ventilation processes can be particularly challenging to model using existing Energy Simulation tools (Zhai, Johnson, and Krarti 2011). Use of a Computational Fluid Dynamics (CFD) model allows direct evaluation of some of the parameters such as window discharge coefficients and convective heat transfer coefficients that must be specified in lumped parameter, airflow network models. Parameterizations in the airflow network models used within Energy Simulation tools have historically been based on experimental data, however detailed CFD simulations can provide a less expensive and more flexible alternative for determining parameter dependencies.

In this study, CFD is used to validate a modified expression for the discharge coefficient for pivoted windows as a function of window angle and aspect ratio. The prediction of ventilation driven by wind or buoyancy is very sensitive to the geometry of vents that constrict the flow path. If

the area and discharge coefficient of these vents are well known, then the airflow rate can often be well-modeled by multi-zone models. Limited information is available, however, on choosing the appropriate discharge coefficient. Here, the discharge coefficient for a horizontally-pivoted window is explored and the same approach could be used to consider a range of inlet geometries. The parameterization in this study refers to an expression that uses the window geometry to relate the discharge coefficient of a pivoted window to that of a rectangular opening of the same width and height. The expression in this study is a function of the window angle and aspect ratio of the pivoted window. The cooling and ventilation capacity due to wind and buoyancy driven flows is strongly dependent on the window discharge coefficient, so the accuracy of the coefficient can have a substantial impact on the ability of a model to predict performance. The modified parameterization presented and validated in this study could be easily included in existing airflow network modeling tools to allow users to determine the discharge coefficient for pivoted windows if the window angle and window aspect ratio are known.

### BACKGROUND

In passively ventilated spaces, key design considerations are the number and size of the vents as well as the resistance to flow along the flow path. Factors that act to reduce flow through the space such as friction and flow contraction are most significant where the cross-sectional area open to the flow is smallest. It is standard practice in airflow network tools to model the effects of friction and flow contraction through large openings using a discharge coefficient. The discharge coefficient is the ratio of the actual flow to the ideal flow:

$$Q = C_d A \sqrt{\frac{2\Delta P}{\rho}}, \quad (1)$$

where  $Q$  is the flow rate through the opening,  $A$  is the area of the opening,  $\Delta P$  is the pressure difference across the opening and  $\rho$  is the fluid density (Irving et al. 2005). More generally, flow through an opening can be modeled

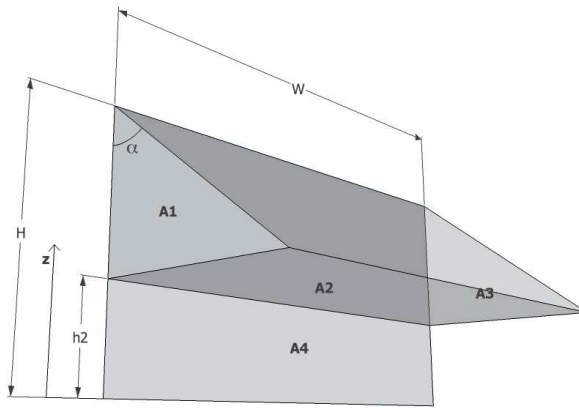


Figure 1: Schematic of window pivoted from the top of the window frame.

with a power law relationship: the flow  $Q$  is proportional to  $\Delta P^n$  where  $n$  approaches 1 in the limit of laminar flow which occurs in narrow cracks, and  $n = 0.5$  in the limit of turbulent flow, which is consistent with Equation 1 (Sherman 1992). An overall discharge coefficient is sometimes used to combine losses along the flow path from the inlet, interior space and outlet into a single parameter. In a typical passively-ventilated space, losses at the smallest opening tend to dominate, but if the flow is routed through ducts in the ceiling or floor this can also have a significant impact on the overall discharge coefficient. In this study  $C_d$ , refers to the discharge coefficient for a specific opening.

For a sharp-edged rectangular orifice, the discharge coefficient is  $C_d = 0.61$ . The discharge coefficient of an orifice does vary to some degree with Reynolds number (White 1999), but previous research shows little variation of the discharge coefficient with Reynolds number for parameters appropriate for building ventilation (Heiselberg, Svdt, and Nielsen 2001). The value  $C_d \approx 0.6$  is often used for rectangular window openings. In the example files provided with the Energy Simulation tool, EnergyPlus, all simple and detailed windows and doors use  $C_d$  varying between 0.5 and 0.6 as the window is opened from 0% to 100%. Previous studies have suggested that the discharge coefficient depends on the temperature difference between the fluids on either side of the orifice, although results differ on the sign and magnitude of the impact (Allard and Utsumi 1992).

Pivoted windows (also known as top-, bottom- or side-hung windows) are very common in buildings but the discharge coefficient for this type of window is not currently well parameterized. Coley (2008) highlights problems in some airflow models with the modeling of top-pivoted windows, specifically at very low angles for buoyancy-driven exchange flows. The pivoted window pane can ob-

struct the flow, leading to a lower flow rate than through a rectangular orifice of the same size. Heiselberg et al. (2001) studied the discharge coefficient for pivoted windows experimentally, however  $C_d$  was calculated using the minimum geometric area open to flow for  $A$  in Equation 1. In practice it is difficult to calculate the minimum area open to air flow, whereas window opening angle and the area open to flow in the vertical plane  $WH$  where  $W$  and  $H$  are the window width and height are straightforward to measure or to specify in a design.

In the pivoted window case, the flow through the window is obstructed by the pane, and it is convenient to use an effective area,  $A_{eff}$ , to describe the equivalent area of the rectangular orifice that would have the same flow  $Q$  as the pivoted window opening. Using this effective area, the discharge coefficient is that of a rectangular opening,  $C_{d,90}$  (i.e., the discharge coefficient of the fully open window,  $\alpha = 90$ ). Rather than using the product  $AC_d$ , where  $A = WH$  and  $C_d$  is the effective discharge coefficient for a window at angle  $\alpha$ , the product of the effective window area and the fixed discharge coefficient  $A_{eff}C_{d,90}$  can be substituted for  $AC_d$  in Equation 1.

In the EnergyPlus Airflow Network Model, the effect of the flow obstruction due to the pivoted pane is included in  $A_{eff}$  by modifying the effective width of the window:

$$W_{pivot} = \left( \frac{1}{W^2} + \frac{1}{(2(H_A - z)\tan(\alpha))^2} \right)^{-1/2}, \quad (2)$$

for  $H_A > z > h_2$ , where  $H_A$  is the axis height,  $\alpha$  is the angle between the pivoted window and the wall, and  $h_2 = H_A(1 - \cos(\alpha))$ , as shown in Figure 1 for a top-pivoted window. For the window shown here, the axis is at the top of the window ( $H_A = H$ ), but some pivoted windows have the axis at an intermediate height (see EnergyPlus 2011). If  $z < h_2$ , (area A4 in Figure 1) the effective width is the full window width,  $W$ . The effective width is integrated over the window height,  $H$ , to get an effective area,  $A_{eff}$  as a function of window angle  $\alpha$ .

In this study, two parameterizations (the one above as well as a modified version) are compared with previous measurements as well as CFD simulations of flow rate through pivoted windows. The airflow model 'MacroFlo' calculates the discharge coefficient for windows based on test data supplied by window manufacturers, according to model documentation (IES 2011). MacroFlo is a multi-zone airflow model included in the energy simulation tool Virtual Environment, developed by Integrated Environmental Solutions Limited (IES), based on the Apache simulation engine. For a pivoted window at a specified angle, the effective discharge coefficient is calculated by interpolating from a data set based on manufacturer test data.

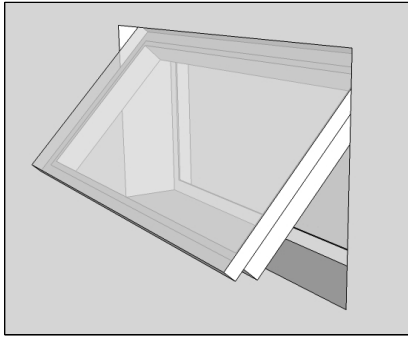


Figure 2: Detailed window geometry as modeled in Fluent.

## METHODS

A CFD test cell is used to examine the dependence of  $A_{eff}$  on inlet geometry. Flow through windows of simple and detailed geometry was simulated at a range of angles and at two window aspect ratios:  $W/H = 0.5$  and  $W/H = 2$ . The simple window geometry simulated in this study is an angled plane extending outward from the top edge of a rectangular opening. Both the wall and window pane have zero thickness. One example of a more detailed window design shown in Figure 2 is also tested in this study. This detailed window model also has a finite wall thickness of 0.18m as shown. These two window types are referred to as 'simple' and 'detailed', respectively. Windows of two aspect ratios were tested over a range of window angles. The static pressure drop through the window is calculated as a function of window angle for the steady-state flow solution. For a constant flow rate  $Q$ , a rectangular orifice with  $A = WH$  will have a pressure drop across the opening:  $\Delta P_{90} = 0.5Q^2\rho/(C_{d,90}A)^2$ , whereas the same flow  $Q$  through a pivoted window at angle  $\alpha$  leads to the pressure drop:  $\Delta P_{\alpha} = 0.5Q^2\rho/(C_{d,90}A_{eff,\alpha})^2$ . The effective area as a fraction of  $A = WH$  can then be calculated:

$$\frac{A_{eff,\alpha}}{WH} = \left( \frac{\Delta P_{90}}{\Delta P_{\alpha}} \right)^{1/2}. \quad (3)$$

The effective discharge coefficient as a function of window angle  $\alpha$  is also calculated from the simulation results using Equation 1 where  $A = WH$  and  $\Delta P$  is taken to be the difference between the face-averaged static pressure at the inlet and outlet of the domain. The domain height was 3.4m and width was 3.6m. Symmetry boundary conditions are imposed along the centerline plane, side wall, top and bottom of the test cell. The upstream face of the test cell serves as a large inlet 5m upstream of the window and the outflow boundary is 5m downstream of the window. The flow rate per vertical opening area  $WH$  was

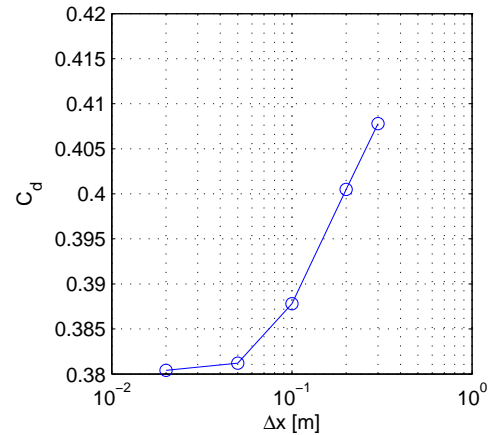


Figure 3: Effect of grid resolution on discharge coefficient. Here, the angle of the pivoted window is  $30^\circ$  and the flow rate is  $0.28\text{m}^3/\text{s}$  through the full window opening (1.2m long by 0.6m high).

held constant for all simulations,  $Q/WH = 0.4\text{m/s}$ , and was imposed by setting a constant velocity across the inlet face. A typical Reynolds number for the flow through the opening is about 20,000.

For the CFD simulations in this study, the Reynolds-Averaged Navier-Stokes equations are solved for steady-state solutions using ANSYS/Fluent. Flow in portions of the domain is expected to be turbulent and so the  $k - \epsilon$  Renormalized Group Theory (RNG) turbulence closure model is used. The RNG model is chosen over the standard  $k - \epsilon$  model because the RNG model does not require the specification of any empirical constants, and in recent studies, the RNG model has been recommended for indoor airflow simulations (Chen 1995; Ji, Cook and Hanby 2007; Zhang and Chen 2007). In this study, the use of the standard  $k - \epsilon$  model lead to very similar results but those are not included here.

The air is modeled as an incompressible, ideal gas. For the window discharge coefficient testing, the fluid density is constant. The effects of compressibility are small for these flows. The model spatial discretization is Green-Gauss cell based with 2nd order upwind discretization for the momentum, turbulent kinetic energy and turbulent dissipation rate and the body force weighted discretization is used for the pressure. The PISO scheme was used for pressure-velocity coupling. For the two equation  $k - \epsilon$  RNG turbulence model, standard wall functions near the wall were used. Under-relaxation factors of 0.3, 1, 1, 0.7, 0.8, 0.8, 1 and 1 were used for pressure, density, body forces, momentum, turbulent kinetic energy, the turbulent dissipation rate, turbulent viscosity, and energy. For the single zone, stack-ventilated case referenced at the end

of this study, the discrete transfer radiation model is used along with 2nd order implicit transient discretization. In this single zone case, the air density is a function of the local air temperature

The test cell was also used to determine the sensitivity of the discharge coefficient to the grid resolution. As shown in Figure 3, the calculated discharge coefficient,  $C_d$  decreases by 7% when the grid size is reduced from 30cm to 5cm. As the grid resolution is increased,  $C_d$  converges to about 0.380. The value of  $C_d$  at 5cm grid resolution is within 0.2% of the value at 2cm, thus it was concluded that grid resolution of 5cm surrounding the window inlet is sufficient.

## RESULTS

For a top-pivoted window, the effective area from CFD simulation results is compared in Figure 4 with the parameterization from EnergyPlus as a function of window angle for a wide window (1.2m wide by 0.6m tall) and a narrow window (0.3m wide and 0.6m tall). The results from the CFD simulations differ by up to a factor of 2 from  $A_{eff}/WH$  as calculated using the EnergyPlus parameterization. In Figure 4, the EnergyPlus parameterization compares more closely with the simulations for the narrow window in (a), but in both cases the parameterization leads to a smaller effective area than the CFD results suggest. Although the agreement between the CFD and EnergyPlus results is better at large angles and presumably at the zero degree limit, the typical operational window angle is well between these limits. The CFD results suggest the actual flow rate through a top-pivoted window may be as much as twice the flow rate predicted by Equation 2.

The effective width  $W_{pivot}$  in Equation 2 is derived as the harmonic mean of the window width  $W$  and 2 times the width of  $A1$  at some height  $z$  in Figure 1. Thus the effective width at height  $z$  will tend toward the smaller value of  $W$  or 2 the width of  $A1 + A3$ . In the case of a wide window where  $W \gg H$ , the effective width at height  $z$  will be the width of  $A1 + A3$ , not accounting for any flow that may enter the window through  $A2$ . The expression for  $W_{pivot}$  is modified here to include flow through the sides ( $A1$  and  $A3$ ) as well as flow from beneath window ( $A2$ ):

$$W_{pivot,mod} = \left( \frac{1}{W^2} + \frac{1}{(2(H_A - z)\tan(\alpha) + \sin(\alpha)W)^2} \right)^{-1/2} \quad (4)$$

If air entering the window opening flowing parallel to the pivoted pane is considered, the additional term,  $\sin(\alpha)W$ , in Equation 4 can be interpreted as the effective width of the component of this flow normal to the rectangular window frame opening. The modified effective width in Equation 4 is integrated over the full window height to get the effective area  $A_{eff}$  of the pivoted window. The

resulting relationship between effective window area and angle shows much better agreement with the CFD results in Figure 4. The effective width as a function of elevation  $z$  was not verified in the CFD simulations, only the overall effective area. The effective width as a function of window height is particularly important for modeling buoyancy-driven exchange flow through pivoted windows in spaces with windows only at a single vertical elevation as noted by Coley (2008).

Also shown in Figure 4 is the effective area from measurements by window manufacturers of flow through top-pivoted windows as provided in the IES MacroFlo documentation. IES lists the effective discharge coefficient by window angle and window aspect ratio, and interpolated values for  $C_d$  are normalized by  $C_{d,90}$  to give  $A_{eff}/WH$ . Close agreement between the modified parameterization, the data from window manufacturers and the CFD tests for the simple angled window geometry suggests that the CFD test cell provides an effective method to determine the effective area of a pivoted window.

Figure 5 shows the discharge coefficient rather than the effective area for the CFD results and manufacturer data, as well as CFD results for the more detailed window design in Figure 2. The geometry of the window in Figure 2 varies somewhat from the idealized pivoted plane in a thin wall surface: both the window pane and the wall have finite thickness. Figure 2 provides one example of a pivoted window design, where windows of this design are typically opened to angles between  $35^\circ$  and  $50^\circ$ . The relationship between window angle and effective discharge coefficient is even more non-linear for this particular detailed window design than for the simple angled window. This may be due to additional flow obstruction at small window angles caused by the wall and window thickness in the detailed window case. When the window is fully open, the discharge coefficient is somewhat higher for the detailed window than for the simple window results, with the manufacturer data falling in between. The finite wall thickness in the detailed window geometry may channel the flow more gradually through the window opening, just as a tapered nozzle has higher discharge coefficient than a sharp-edged orifice of the same opening size. This result suggests that wall thickness may need to be considered when determining the discharge coefficient, but the effect of wall thickness is not explored in detail in this study.

## SINGLE ZONE SIMULATION

The parameterization choice for the effective inlet window area (or discharge coefficient) can have a significant impact on the predicted performance of passive ventilation and cooling strategies. To demonstrate the impact of the discharge coefficient, night flush (passive economizer) cooling was simulated in a single building zone as seen in Figure 6. The single zone room had a concrete slab floor

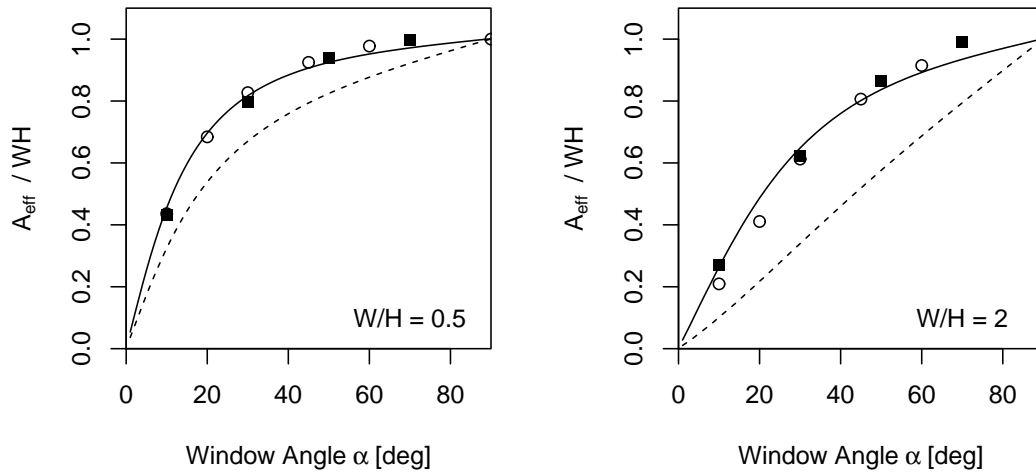


Figure 4: Effective area  $A_{eff}$  for top-pivoted windows scaled by  $WH$ , for (a) narrow window, and (b) wide window from the original (---) and modified (—) EnergyPlus parameterizations, CFD test results for the simple window (■), and measured data reported by IES MacroFlo (o).

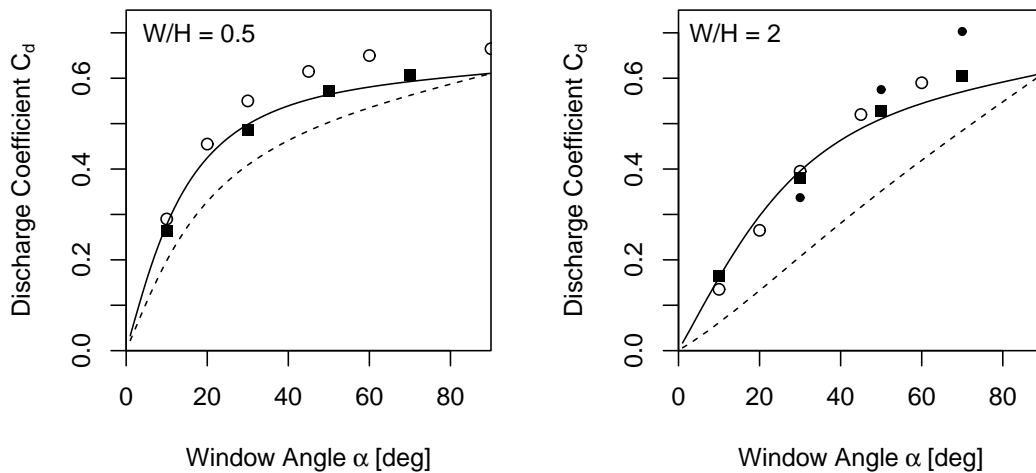


Figure 5: Discharge coefficient for top-pivoted windows for (a) narrow window, and (b) wide window from IES MacroFlo data (o), CFD test results for the simple window (■) and the detailed window geometry (●). The original (---) and modified (—) EnergyPlus parameterizations are shown assuming  $C_{d,90} = 0.61$ .

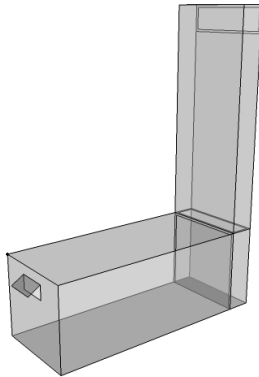


Figure 6: Schematic of Single Zone example case simulated in EnergyPlus and CFD. A pivoted inlet window is on the left of the room zone and at the far end is a stack exhaust with an outlet near the top.

and buoyancy-driven ventilation enters through a pivoted window and is exhausted through a tall stack with a large outlet. The single zone was initialized at a constant temperature above the outdoor temperature and then during the simulation the temperature of the indoor air and thermal mass gradually approaches the outdoor temperature as indoor-outdoor temperature difference drives the stack ventilation. This single zone was simulated using CFD and EnergyPlus with the set-up matched as closely as possible between the two models.

Using the original parameterization in EnergyPlus to determine  $C_d$ , the EnergyPlus simulation of the single zone predicted 38% less heat flushed from the building than the CFD simulation of the same space. However, when the discharge coefficient in the EnergyPlus model was specified according to CFD results from the previous section, the agreement between the two models was dramatically better (the CFD model predicted 7% more heat flushed during the first 10 hours than the EnergyPlus model). Using the modified parameterization in Equation 4 to calculate the discharge coefficient for the inlet window, in this example  $C_d$  is 2.3 times larger than the value calculated by the original formulation used in EnergyPlus. Outdoor obstructions and internal partitions can add to the overall resistance to flow along the path of the passive ventilation, but the resistance to flow (and thus the overall discharge coefficient) is typically dominated by the inlet vent geometry (or outlet vent, whichever has smaller area).

With careful attention to the input parameters, this example suggests that airflow network models can replicate the bulk temperature evolution behavior seen in CFD simulation of buoyancy-driven ventilation in simple spaces. Detailed comparison of EnergyPlus and CFD simulations of buoyancy driven ventilation will appear in a forthcom-

ing study. The impact of the discharge coefficient on the passive cooling capacity will depend on the design of a particular building (including thermal mass, window size and angle), so this example is provided only as a point of reference. This example demonstrates that the predicted performance of passive and mixed-mode ventilation strategies are quite sensitive to the discharge coefficient and window area of vents.

## SUMMARY

Detailed CFD simulations can provide a flexible tool to parameterize geometry and flow-specific coefficients, specifically discharge coefficients through openings. The existing formula used in EnergyPlus to calculate the effective area of pivoted windows tends to under-predict the flow rate through the opening by up to 50%. A modification to this expression is proposed that takes into account the airflow through the sides as well as the bottom of an open, horizontally-pivoted window. Both CFD results and data from window manufacturers agree well with the modified formula and the recommendation is that this new formula be included in airflow network models. The current pivoted window parameterization used in airflow network models such as EnergyPlus may underestimate the cooling capacity for passive ventilation by up to 50%.

## ACKNOWLEDGEMENT

This research was completed at Stanford University and was funded by a grant from the Precourt Energy Efficiency Center.

## REFERENCES

- Allard, F., and Y. Utsumi. 1992. "Airflow through large openings." *Energy and Buildings* 18 (2): 133–145.
- Chen, Q. 1995. "Comparison of different ke models for indoor air flow computations." *Numerical Heat Transfer Part B Fundamentals* 28 (3): 353–369.
- Coley, D.A. 2008. "Representing top-hung windows in thermal models." *International Journal of Ventilation* 7 (2): 151–158.
- EnergyPlus. 2011. *Engineering Reference*. Department of Energy, US.
- Heiselberg, P., K. Svidt, and P.V. Nielsen. 2001. "Characteristics of airflow from open windows." *Building and Environment* 36 (7): 859–869.
- IES: Integrated Environmental Solutions Limited. 2011. *MacroFlo Calculation Methods Manual*. Virtual Environment (VE) Version 6.4.
- Irving, S., B. Ford, and D. Etheridge. 2005. *Natural ventilation in non-domestic buildings, CIBSE AM10*. Page Bros.



- Ji, Y., M.J. Cook, and V. Hanby. 2007. "CFD modelling of natural displacement ventilation in an enclosure connected to an atrium." *Building and Environment* 42 (3): 1158–1172.
- Sherman, M. 1992. "A power-law formulation of laminar flow in short pipes." *Journal of Fluids Engineering* 114 (4): 601–605.
- White, F.M. 1999. *Fluid Mechanics*. McGraw-Hill, New York.
- Zhai, Z., M.H. Johnson, and M. Krarti. 2011. "Assessment of natural and hybrid ventilation models in whole-building energy simulations." *Energy and Buildings* 43 (9): 2251–2261.
- Zhang, Z., W. Zhang, Z. Zhai, and Q. Chen. 2007. "Evaluation of various turbulence models in predicting airflow and turbulence in enclosed environments by CFD: Part 2-Comparison with experimental data from literature." *HVAC and R Research* 13 (6): 871–886.

## NOMENCLATURE

$Q$	flow rate through window
$C_d$	discharge coefficient
$A$	opening area
$\Delta P$	static pressure drop across window
$\rho$	fluid density
$W$	width of window opening
$H$	height of window opening
$W_{pivot}$	effective window width
$H_A$	height of pivot axis
$z$	height
$\alpha$	window angle
$h_2$	height of bottom of pane
$A_{eff}$	effective window opening area
$H$	height of window opening
$W_{pivot}$	effective window width